Mechanical Characterization of Parts Processed via Fused Deposition

Bertoldi M., Yardimci M. A., Pistor C. M., Güçeri S. I., Sala G.
University of Illinois at Chicago

ABSTRACT

The possibility of using materials with better physical and mechanical properties together with the quickly improving capabilities of various processes increasingly make Rapid Prototyping (RP) as a new manufacturing technology for specialty components.

In Fused Deposition Modeling (FDM), the build orientation and the toolpath used strongly affect the properties of the part. This study presents the results of experimental work based on mechanical characterization of parts fabricated with fused deposition to determine the stiffness matrix and the thermal expansion coefficients for an equivalent orthotropic material. The results can be directly adapted into computational analysis tools based on classical lamination theory, for part quality and performance prediction. Current investigation focuses on use of ABS material in Stratasys FDM 1650 rapid prototyping equipment.

BACKGROUND

For conventional polymer-based material technologies the properties of the fabricated parts are well known and can be predicted and determined with different tools and characterization techniques. However, for parts fabricated using rapid prototyping, there are no standard methods available. In the current work, complete mechanical characterization for ABS parts with a pseudo-isotropic stacking sequence has been performed.

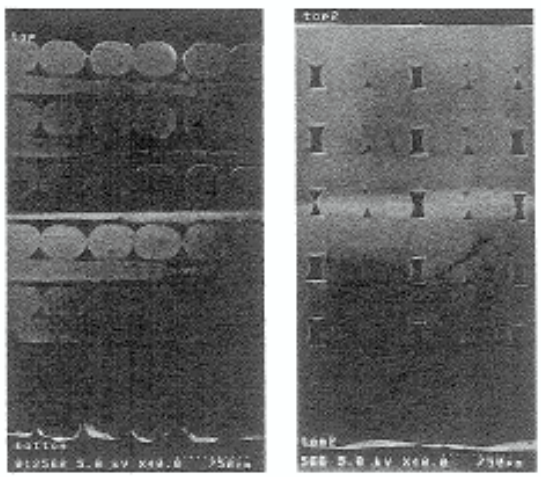

Figure 1 *SEM pictures of a section of a standard lay-up part* [0 90] **[1]**

Fused Deposition process produces a 3D part by superimposing a specified number of layers, where each of them is generated by parallel roads. The internal microstructure can be assimilated to a composite two-phase material, where the roads correspond to fibers (**Figure 1**). Weak bonding between the roads and voids, coupled with inherently anisotropic properties of extruded roads enhance this similarity and make the local orthotropic behavior more pronounced.

Similar to a standard polymeric matrix composite, the FDM parts can be assumed to be linear, elastic and orthotropic. The general strain-stress relation (see [1] for details) for an orthotropic material is:

$$\begin{bmatrix} \varepsilon_1 \\ \varepsilon_2 \\ \varepsilon_3 \\ \gamma_{23} \\ \gamma_{13} \\ \gamma_{12} \end{bmatrix} = \begin{bmatrix} S_{11} & S_{12} & S_{13} & 0 & 0 & 0 \\ & S_{22} & S_{23} & 0 & 0 & 0 \\ & & S_{33} & 0 & 0 & 0 \\ & sym. & & S_{44} & 0 & 0 \\ & & & & S_{55} & 0 \\ & & & & & S_{66} \end{bmatrix} \bullet \begin{bmatrix} \sigma_1 \\ \sigma_2 \\ \sigma_3 \\ \tau_{23} \\ \tau_{13} \\ \tau_{12} \end{bmatrix} \tag{1}$$

The [6x6] compliance matrix can be inverted it to obtain the stiffness matrix:

$$\begin{bmatrix} \varepsilon_1 \\ \varepsilon_2 \\ \varepsilon_3 \\ \gamma_{23} \\ \gamma_{13} \\ \gamma_{12} \end{bmatrix} = \begin{bmatrix} \frac{1}{E_1} & \frac{-\nu_{21}}{E_2} & \frac{-\nu_{31}}{E_3} & 0 & 0 & 0 \\ & \frac{1}{E_2} & \frac{-\nu_{32}}{E_3} & 0 & 0 & 0 \\ & & \frac{1}{E_3} & 0 & 0 & 0 \\ & & & \frac{1}{G_{23}} & 0 & 0 \\ & sym. & & & \frac{1}{G_{13}} & 0 \\ & & & & & \frac{1}{G_{12}} \end{bmatrix} \bullet \begin{bmatrix} \sigma_1 \\ \sigma_2 \\ \sigma_3 \\ \tau_{23} \\ \tau_{13} \\ \tau_{12} \end{bmatrix} \tag{2}$$

In order to determine nine independent constants it is necessary to test six different specimens. The elastic modulus can be obtained from the stress-strain diagram:

$$E_x = \frac{\Delta \sigma_x}{\Delta \varepsilon_x} \tag{3}$$

Poisson ratio is defined as:

$$\nu_{xy} = \frac{-\varepsilon_y}{\varepsilon_x} \tag{4}$$

In-plane shear modulus G can be obtained from the test of a 45° oriented bar, as follows:

$$G_{ab} = \frac{E_x}{2(1+\nu_{xy})} \tag{5}$$

where x and y are the direction of load application and the normal direction respectively. Also, a and b correspond to 1 and 2 for the specimen in the xy plane, 2 and 3 for the one in the xz plane and 3 and 1 for the one in the yz plane.

If we also consider an externally applied temperature variation, and assuming that the free thermal strain is linearly dependent on temperature, the stress-strain equations take the form:

$$\begin{bmatrix} \varepsilon_1 - \alpha_1 \Delta T \\ \varepsilon_2 - \alpha_2 \Delta T \\ \varepsilon_3 - \alpha_3 \Delta T \\ \gamma_{23} \\ \gamma_{13} \\ \gamma_{12} \end{bmatrix} = \begin{bmatrix} S_{11} & S_{12} & S_{13} & 0 & 0 & 0 \\ & S_{22} & S_{23} & 0 & 0 & 0 \\ & & S_{33} & 0 & 0 & 0 \\ & sym. & & S_{44} & 0 & 0 \\ & & & & S_{55} & 0 \\ & & & & & S_{66} \end{bmatrix} \bullet \begin{bmatrix} \sigma_1 \\ \sigma_2 \\ \sigma_3 \\ \tau_{23} \\ \tau_{13} \\ \tau_{12} \end{bmatrix} \tag{6}$$

and consequently the inverse relations (3) becomes:

$$\begin{bmatrix} \sigma_1 \\ \sigma_2 \\ \sigma_3 \\ \tau_{23} \\ \tau_{13} \\ \tau_{12} \end{bmatrix} = \begin{bmatrix} C_{11} & C_{12} & C_{13} & 0 & 0 & 0 \\ & C_{22} & C_{23} & 0 & 0 & 0 \\ & & C_{33} & 0 & 0 & 0 \\ & sym. & & C_{44} & 0 & 0 \\ & & & & C_{55} & 0 \\ & & & & & C_{66} \end{bmatrix} \bullet \begin{bmatrix} \varepsilon_1 - \alpha_1 \Delta T \\ \varepsilon_2 - \alpha_2 \Delta T \\ \varepsilon_3 - \alpha_3 \Delta T \\ \gamma_{23} \\ \gamma_{13} \\ \gamma_{12} \end{bmatrix} \tag{7}$$

Eq. (7) represents the complete constitutive relation for an orthotropic material.

TEST SETUP

The experimental testing has been conducted using the procedure explained in [3] and [4], on a INSTRON 5569 machine, with the following equipment:

- a cross-head screw-driven by a DC servo motor, with a speed range of 0.001 to 500 mm/min.
- a load cell with a maximum load capacity of ± 50 KN.
- two wedge action grips
- one axial strain extensometer with a gauge length of 50 mm
- one transverse strain extensometer with a gauge length of 10 mm

PREPERATION OF TENSILE TEST BARS

The specimens for the tensile tests were designed according to the specifications of the ASTM D 5937-96 standard for molded plastic parts [5], since no special standard exists for the

characterization of RP parts. The bar was designed using Pro/Engineer and exported in the STL format. Using QuickSlice 5.0, it was oriented in six different ways (**Figure 2**) and then sliced. The vertical and the 45° oriented bars in the *xy* and *zy* planes were built with the "contain support" option (the entire part is surrounded by support).

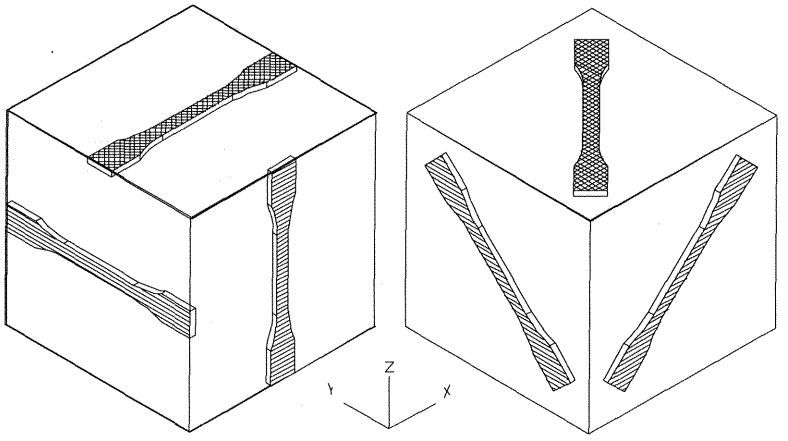

Figure 2 *Test specimen orientation*

The properties of the layers have been set to obtain a road orientation variable in the *z* direction with the pseudo-isotropic stacking sequence:

[0 90 +45 -45]

RESULTS

For every specimen the following data have been collected:

- Ultimate tensile strength
- Elastic (Young's) modulus
- Poisson ratio

The Young's modulus has been calculated from the stress-strain diagram (Eq. 3); a MATLAB function has been implemented to perform a least square interpolation of the linear portion of the curve. The same has been done to calculate the Poisson ratio (4), which is the ratio between the slopes of the two curves (stress-axial strain and stress-transverse strain). The data reduction of the results presented some difficulties due to the scattered values obtained; small variations of the processing parameters can strongly affect the measurements. Premature failure of the specimens was caused by different reasons:

- Intralaminar defects, due to presence of excess material stuck to the nozzle and then dropped onto the layer
- Interlaminar defects due to over or under fill between rasters or between rasters and contour
- Surface roughness (initiation of microcracks)

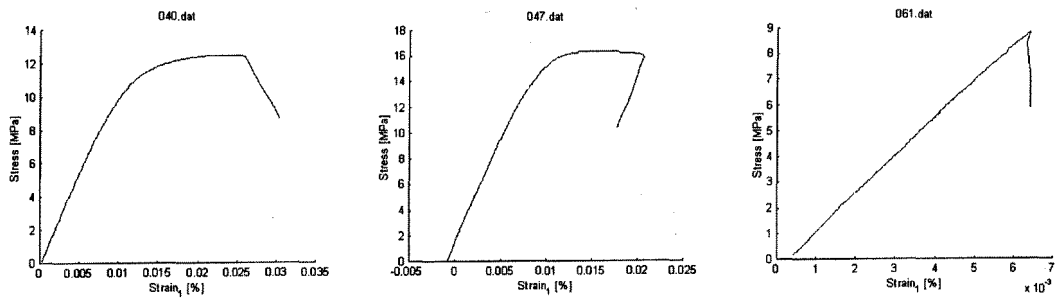

(a) (b) (c)

Figure 3 *Stress – strain curves for x-y (a), y-z (b) and x-z (c) oriented specimens.*

The first point has been particularly critical for the vertical (*x-z*) bar, because of the large number of layer (> 600), causing in all the specimens a brittle failure (**Figure 3-c**). In some tests the failure occurred close to the grips, and the results had to be discarded. The parts in the *x-y* and *y-z* planes presented a common elasto-plastic behavior (**Figure 3-a** and **Figure 3-b**); however, it must be noticed as the *y-z* part resulted in the highest value for both the elastic modulus and the tensile strength. The *xz* part has the lowest tensile strength (**Figure 4**). All the results are presented in **Table 1**.

Toolpath	Build plane	Orientation	Number of specimens tested	Number of specimens considered	Avg.tensile strenght [MPa]	Avg. elastic modulus [MPa]
[0 90 +45 –45]	xy	X	4	4	11.700	1072.900
[0 90 +45 –45]	yz	Y	4	4	15.987	1652.523
[0 90 +45 –45]	xz	Z	11	6	7.608	1391.448
[0 90 +45 –45]	xy	x+45	5	5	10.808	970.944
[0 90 +45 –45]	yz	y+45	5	4	13.465	1519.115
[0 90 +45 –45]	xz	z+45	3	3	14.702	1527.600

Table 1 *Tensile test results*

Finally, the stiffness matrix is obtained as:

$$C = 1.0e+003 * \begin{bmatrix} 1.8530 & 1.4348 & 1.1810 & 0 & 0 & 0 \\ 1.4348 & 3.0843 & 1.6444 & 0 & 0 & 0 \\ 1.1810 & 1.6444 & 2.4141 & 0 & 0 & 0 \\ 0 & 0 & 0 & 0.5540 & 0 & 0 \\ 0 & 0 & 0 & 0 & 0.5405 & 0 \\ 0 & 0 & 0 & 0 & 0 & 0.3696 \end{bmatrix}$$

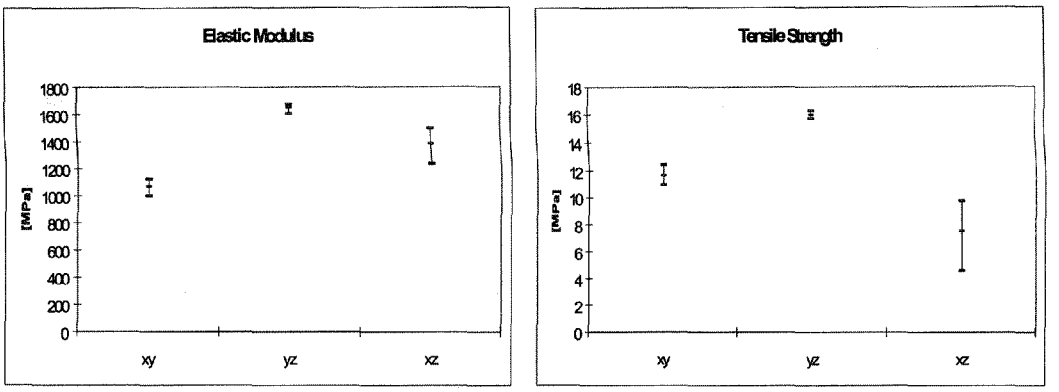

Figure 4 *Max, min and avg. values of elastic modulus (a) and tensile strength (b).*

THERMAL EXPANSION

To calculate the three thermal expansion coefficients, a series of tests has been conducted; three square specimens have been built with the same stacking sequence of the tensile test bars ([0 90 +45 -45]). **Figure 5** shows the specimens built, for which the dimensions can be found in **Table 2**. The test procedure is presented in [3].

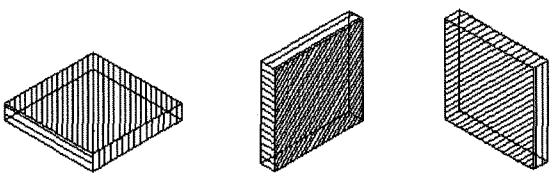

Figure 5 *Thermal expansion specimens*

The test setup consists of:

- A Scientific Inc. VWR 1410 oven.
- A Power Macintosh equipped with a Lab NB Data Acquisition Board and LabVIEW Software for data acquisition and processing.
- Strain gages and thermocouples.

The technique employed [6] uses two well-matched strain gages, one bonded to a specimen of the reference material (glass, which was considered to have isotropic thermal expansion coefficient) and the other to the specimen of the test material. The temperature range is 0 to 150 °C. Under stress-free environment, the differential output between the two gages, at

any common temperature, is equal to the differential unit expansion. One of the many advantages of using strain gages for measuring thermal expansion coefficient is the possibility to determine expansion coefficients in one direction. The electrical circuit employed is depicted in **Figure 6**.

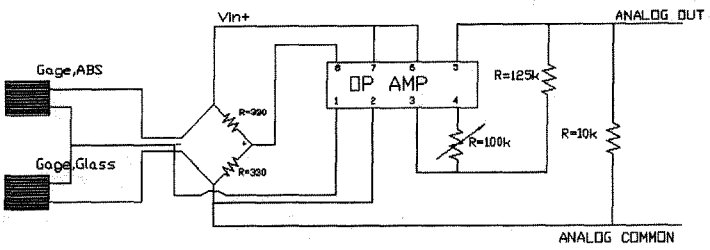

Figure 6 *Strain gages circuit*

The electrical output of the circuit is due to the combined resistance changes from both sources (ABS and glass specimens). The net resistance change can be expressed as the sum of resistivity and differential expansion effects as follows:

$$\frac{\Delta R}{R} = \left[\beta_G + (\alpha_S - \alpha_G) F_G\right] \Delta T \tag{8}$$

where:

- $\frac{\Delta R}{R}$ = unit resistance change
- β_G = thermal coefficient of resistivity of grid (strain gage) material
- $\alpha_S - \alpha_G$ = difference in thermal expansion coefficients between specimen and grid, respectively
- F_G = gage factor of the strain gage
- ΔT = temperature change from arbitrary initial reference temperature

To calculate the strain due to a resistance change the following formula can be used:

$$\varepsilon = \frac{\Delta R / R}{F_G} \tag{9}$$

Therefore, substituting $\frac{\Delta R}{R}$ into equation (8) we have:

$$\varepsilon_{G/S} = \left[\frac{\beta_G}{F_G} + (\alpha_S - \alpha_G)\right] \Delta T \tag{10}$$

where $\varepsilon_{G/s}$ is the thermal output for grid alloy G of the test specimen.

By introducing glass (reference material) and deriving the thermal output $\varepsilon_{G/g}$ from a half Wheatstone bridge configuration, the effect of the grid material resistivity $\frac{\beta_G \Delta T}{F_G}$ is eliminated. The thermal expansion coefficient can be finally obtained:

$$\alpha_s = \alpha_g + \frac{\varepsilon_{(s-g)}}{\Delta T} \tag{11}$$

where:

$$\varepsilon_{(s-g)} = \varepsilon_{G/s} - \varepsilon_{G/g} \tag{12}$$

To find an actual strain $\varepsilon_{(s-g)}$ an expression for Wheatstone bridge was used as:

$$\frac{V_o}{V} = \frac{F_G \varepsilon_{(s-g)} * 10^{-6}}{4 + 2F_{(G)} \varepsilon_{(s-g)} * 10^{-6}} \tag{10}$$

where V_0= Voltage output [V] and V = Voltage input [V].

RESULTS

Different values for the thermal expansion coefficient of molded ABS can be found in literature: 80 and 130 $*10^{-5}$ [m/m*C^{-1}] for Bayer's ABS (Novodur), 78 and 105 $*10^{-5}$ [m/m*C^{-1}] [4], 62 and 130 $*10^{-5}$ [m/m*C^{-1}] (standard molded, medium impact ABS).

All the values measured are at the lower boundary of the available data; this can be explained considering the voids existing between the roads, which allow expansion within the layers. It can also be observed how the vertical specimen presents the largest thermal expansion coefficient, due to the lower content of intralaminar voids. The results are presented in **Table 2**.

Build plane	Build direction	Number of specimens tested	Number of specimens considered	Width [mm]	Length [mm]	Thickness [mm]	Number of layers	Thermal expansion coefficient
xy	x	2	2	50	50	5.3	20	4.785E-05
yz	y	1	1	50	50	5.3	197	6.475E-05
xz	z	1	1	50	50	5.3	197	7.697E-05

Table 2 *Thermal expansion results*

CONCLUSIONS

The results of the experimental work conducted show the build orientation strongly affects the tensile strength, the elastic modulus and the thermal expansion coefficient of parts processed via Fused Deposition Modeling. The stiffness matrix obtained can be directly utilized for prediction and analysis purposes.

This work is of particular importance as Fused Deposition Modeling evolves from a Rapid Prototyping to a Rapid Manufacturing process. Future research will be focused on:

- Application of similar analysis to other materials and processes.
- Integration of part properties prediction model in the design phase.

REFERENCES

1. Takeshi Hattori, private comunications, Mitshubishi Chemicals, 1998
2. Stress analysis of fiber reinforced composite materials, Michael W. Hyer, WCB/McGraw-Hill 1997
3. Experimental Characterization of Advanced Composite Materials, Leif A. Carlsson - R. Byron Pipes, Prentice-hall,INC, Englewood Cliffs, New Jersey 07632 1987
4. Handbook of Plastics Testing Technology, Vishu Shah, John Wiley & Sons 1984
5. D5937-96 Standard Test Method for Determination of Tensile Properties of Moulding and Extrusion Plastics, American Society for Testing and Materials, Conshohocken, PA. 1997
6. Measurement of Thermal Expansion Coefficient, Measurements Group Tech Note TN-513-1 1994